Sensors and Actuators A 161 (2010) 322–328

Contents lists available at ScienceDirect

Sensors and Actuators A: Physical

journal homepage: www.elsevier.com/locate/sna

RF evanescent-mode cavity resonator for passive wireless sensor applications

Yanzhu Zhao[a,*], Yuan Li[a], Bo Pan[a], Seong-Hyok Kim[a], Zhan Liu[b], Manos M. Tentzeris[a], John Papapolymerou[a], Mark G. Allen[a]

[a] School of Electrical and Computer Engineering, Georgia Institute of Technology, United States
[b] School of Polymer, Textile and Fiber Engineering, Georgia Institute of Technology, United States

ARTICLE INFO

Article history:
Received 17 September 2009
Received in revised form 14 April 2010
Accepted 15 April 2010
Available online 6 May 2010

Keywords:
Passive wireless sensor
Evanescent-mode cavity resonator
Airflow
Antenna

ABSTRACT

This paper presents a radio-frequency (RF) evanescent-mode cavity resonator for passive wireless sensor applications. The evanescent-mode resonator is composed of a cavity with a center post. The resonant frequency of the resonator is determined by the dimension of the cavity, the gap between top membrane electrode of the cavity, and the center post. In a wireless airflow sensor application proposed in this paper, the top electrode of the cavity resonator is deformed when airflow is applied. This results in a resonant frequency shift. A coplanar waveguide (CPW) coupling method has also been proposed for the sensor structures. The proposed coupling method has demonstrated low transition loss with a relatively simplified signal feeding structure, resulting in easy integration of sensing elements and RF antenna. The fabrication of the proposed flow sensor is realized by a simple molding technology. Measurements of airflow velocity using the proposed flow-sensor have been demonstrated with sensitivity of 0.37 GHz/(m/s). Passive wireless interrogation has also been achieved by integrating the sensor with a pair of ultra-wide-bandwidth (UWB) antennas.

Published by Elsevier B.V.

1. Introduction

There is a growing need for wireless sensing for medical/clinical applications, structural health monitoring, and mission-critical industrial and military applications [1,2]. Passive wireless sensors do not require onboard power supply or active circuits. Thus, these sensors are especially useful in harsh environmental and embeddable sensing applications, where active components cannot work properly, or the onboard batteries cannot be replaced non-invasively. Passive wireless sensors are generally composed of resonant circuits with lumped discrete elements and antennas/loops. In the passive wireless sensor, the sensing element is integrated into the resonant circuits, and the change of resonant frequency can be wirelessly detected. Most common wireless passive sensors are based on inductive coupling at LF and HF bands [3–5]. They are usually compact in size and easy to fabricate. However the signal-to-noise ratio is limited by relatively low *Q*, and the interrogation is typically constrained to very near field. Another type of passive wireless sensor utilizes a surface-acoustic-wave (SAW) resonator [6], which has high *Q* and is very sensitive to the surface properties such as pressure or temperature, when it is integrated into appropriate mount and package [7]. Passive wireless sensors using high *Q* radio-frequency (RF) waveguides have also been reported for embedded wireless strain monitoring [8]. The strain sensor uses a conducting coaxial RF cavity, and the changes in the dimensions reflect in the shift of the resonant frequency. However, the waveguide is bulky in size, and the attachment of external antenna further increases size and complexity.

It is possible to exploit wireless sensors in the microwave and millimeter wave range due to rapid advances in low cost GHz electronics and circuits. Unlike crowded HF and UHF bands, the microwave and millimeter wave portion of the RF spectrum remains much less occupied by commercial wireless applications. Besides, the energy propagation characteristics at these frequencies potentially enable many benefits such as excellent immunity to interference and high security, resulting in significant reduction of the complexity and cost of the sensing system. However distributed elements such as transmission lines must be used at this frequency range and are challenging for design.

Evanescent-mode cavity resonators inherently fulfill the need for wireless sensor applications, because the size is greatly reduced compared with regular cavity resonators and the sensitivity of the resonant frequency as a function of the cavity dimension becomes more pronounced. Evanescent-mode cavity resonators with tunable resonant frequencies have been demonstrated recently in RF filter applications [9–13]. An evanescent-mode cavity resonator based micro-electro-mechanical-system (MEMS) thermal sensor has also recently been demonstrated using stereolithography process [14]. The batch fabrication of these air-lifted RF components such as air cavity or waveguide, as well as the feeding structures

* Corresponding author. Tel.: +1 952 446 5691.
E-mail address: yzhao@gatech.edu (Y. Zhao).

0924-4247/$ – see front matter. Published by Elsevier B.V.
doi:10.1016/j.sna.2010.04.017

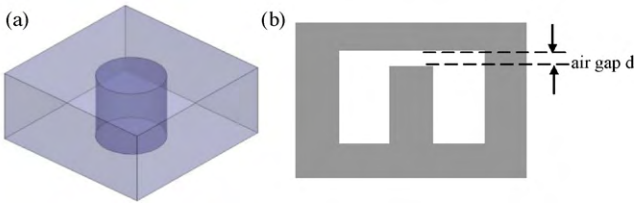

Fig. 1. Schematic of evanescent-mode cavity resonator: (a) lateral view and (b) cross-sectional view.

are usually achieved by surface micromachining or silicon DRIE [15,16]. However, due to the complexity of the fabrication and the feeding structures it has been challenging to integrate the sensing elements. These challenges have limited the application of the previously reported MEMS sensors to wireless interrogation.

In this paper, a wireless passive sensing technique based on a CPW-fed evanescent-mode cavity resonator is presented. The process for the proposed sensor is be based on the micro-molding of thermoplastic polymers reported in our previous papers [17–19], which have demonstrated a low-cost implementation of air-lifted radio-frequency components and the cavity resonators with unloaded Q of greater than 500 [18]. A simple coplanar waveguide (CPW) feeding structure is utilized to excite the resonance mode and enables an easy integration of sensing elements as well as the antenna. The CPW feeding structure is formed simultaneously during the molding process using a metal transfer technique. The wireless interrogation of the sensor is also demonstrated.

2. Sensor concept

A rectangular or circular cavity resonator has a dimension on the order of a half-wavelength, while the evanescent-mode cavity resonator can have much smaller size with the same resonant frequency [9–11,19]. Fig. 1 shows a schematic of an evanescent-mode cavity resonator. It is composed of a rectangular or circular cavity with an electrically shorted center post. When the air gap (d) closes to zero, the resonant frequency drops quickly thanks to the increased parasitic capacitance between the cavity and the post. Therefore, the resonant frequency can be determined approximately by the following equation [9–12]:

$$\omega \approx \frac{1}{\sqrt{LC_{post}}} \tag{1}$$

where L is equivalent inductance related to the surface current, and C_{post} is the capacitance between the top surface of the post and the top electrode of the cavity. C_{post} is the dominant capacitance of the resonator when the air gap is far smaller than the cavity dimension

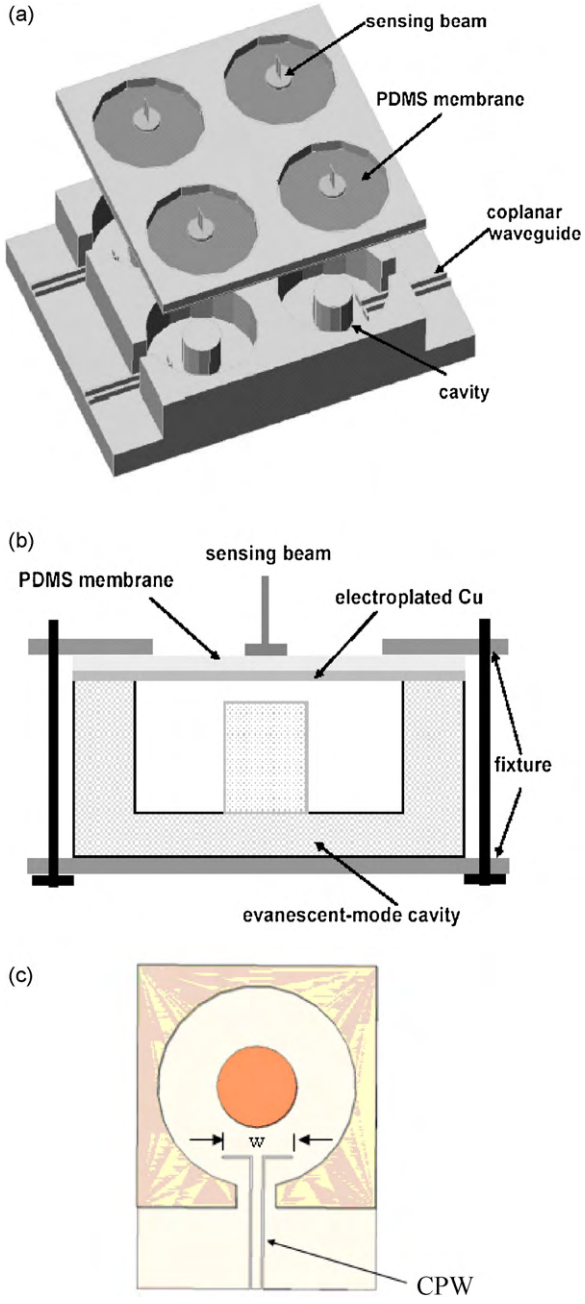

Fig. 3. Design schematic of the airflow sensor array: (a) lateral view, (b) cross-sectional view, and (c) top view of one resonator unit.

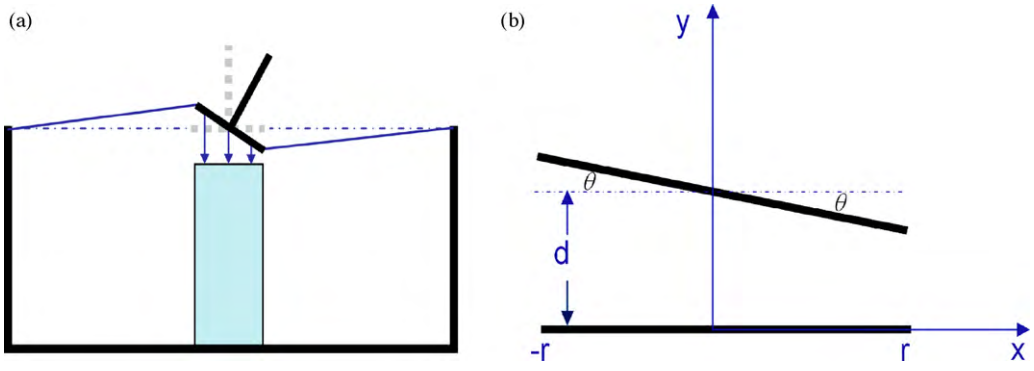

Fig. 2. Schematic of the airflow sensor mechanism: (a) sensor mechanism and (b) equivalent capacitance model.

and can be calculated as:

$$C_{post} = \frac{\varepsilon_r \varepsilon_0 A}{d} \tag{2}$$

3. Airflow sensor

To prove the proposed sensing mechanism, an evanescent-mode resonator sensor for measuring airflow velocity based on the tangential sensing concept is designed and demonstrated. Fig. 2 shows the operation principle of the airflow sensor based on the evanescent-mode cavity resonator. An elastic membrane seals the cavity, and a miniature sensing beam protrudes from the membrane surface and extends into the flow in order to effectively sense the mean-free stream velocity of the airflow. The beam is deflected by the airflow, changing the capacitance between the elastic membrane of the cavity and the top surfaces of the post and, thereby, the resonance frequency of the cavity resonator.

For a small beam deflection angle θ ($\sin\theta \approx \theta$), the equivalent capacitance and resonance frequency of the resonator can be calculated from:

$$C' = \int_{-r}^{r} \varepsilon_0 \frac{\Delta A}{d - x\theta}, \tag{3a}$$

where ΔA is the area of the parallel plate for Δx length, d is the air gap between the top surfaces of the cavity and post, r is the radius of the capacitive post, then:

$$C' \approx C \frac{s}{2\theta} \ln\left(\frac{s+\theta}{s-\theta}\right) \tag{3b}$$

$$f_r = f_0 \sqrt{\frac{C}{C'}} = \frac{1}{\sqrt{s/2\theta \ln((s+\theta)/(s-\theta))}}, \tag{4}$$

where $s = d/r$, and C and C' are the equivalent capacitance of the resonator before and after the beam deviation; f_0 and f_r are the resonant frequencies before and after shifting. Please note the above equations are a good approximation only for small deflection angle θ, more accurate analysis can be found in [9–11].

Fig. 3 shows the design schematic of a 2 × 2 airflow sensor array based on the evanescent-mode circular cavity resonator. The sensor is assembled by two main parts including the RF structure (cavity and CPW) and mechanical structure (membrane and sensing beam). Polydimethylsiloxane (PDMS) elastomer is utilized for the membrane structure and is coated with a thin layer (3 μm) of copper for electrical functionality. The cavity resonator and sensing elements are fabricated separately and assembled using a small plastic fixture. A simple CPW feeding structure is designed to excite the cavity resonance as in Fig. 3(c). The opening on the sides of cavity is in parallel with the current path to minimize the effects on the resonance. At a certain width of the CPW split-end structure, a critical coupling from the CPW to the evanescent-mode cavity resonator can be achieved [12–14,18]. Based on the simulation, the width of the CPW center conductor and the width of the slot between the signal and the ground are designed to be 0.18 and 0.05 mm, respectively. The insertion end of the CPW has a split slot structure with an arm of 0.9 mm at each end. Table 1 shows the designed parameters for a cavity resonator with a resonant frequency of 14 GHz.

Table 1
Design parameters of cavity resonators for airflow measurement.

	Cavity radius	Cavity height	Post radius	Post height
Cavity design	2.00 mm	2.50 mm	0.75 mm	2.40 mm

Metal-transfer-molding (MTM) technique is utilized when fabricating the cavities [17,18]. The mold master is made by stereolithography (SLA) and can be repetitively used for continuous molding processes. The seed layer (Au/Ti) is pre-patterned on PDMS mold and transferred to molded polymers to form the metallized 3-D structures and the CPW feeding lines simultaneously. Copper electroplating is performed to thicken the metal coating. Fig. 4(a) shows the fabricated cavity resonator array using the MTM process. The CPW feeding structures are inserted into the cavity through a small opening on the side of the cavity. Fig. 4(b) shows the fabricated sensor, which was assembled using a plastic fixture. A 50 μm thick elastic membrane is fabricated by spin-coating PDMS solution, followed by thermal curing. The elastic nature of the PDMS membrane enables a high-strain–stress ratio. The thin copper layer is formed by sputtering on the membrane surface and reinforced by electroplating. The membrane is bonded on the top of the cavity by a fixture. A 3 mm long plastic beam is then bonded on the top of the cavity to facilitate the measurement.

The sensitivity of the sensor can be expressed as

$$S = \frac{\Delta f_r}{\Delta v_{airflow}} = \frac{\Delta f_r}{\Delta \theta_{beam}} \cdot \frac{\Delta \theta_{beam}}{\Delta v_{airflow}} = S_{RF} \cdot S_{mechanical}, \tag{5}$$

where

$$S_{RF} \equiv \frac{\Delta f_r}{\Delta \theta_{beam}} \tag{6}$$

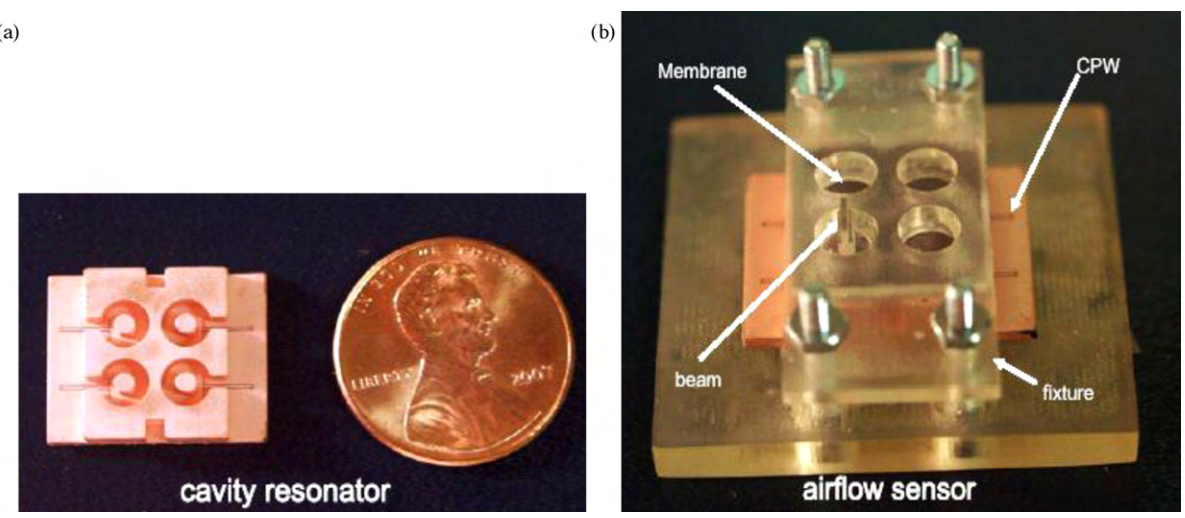

Fig. 4. Fabricated airflow sensor array: (a) fabricated evanescent-mode cavity resonator array by MTM process and (b) assembled airflow sensor by fixture.

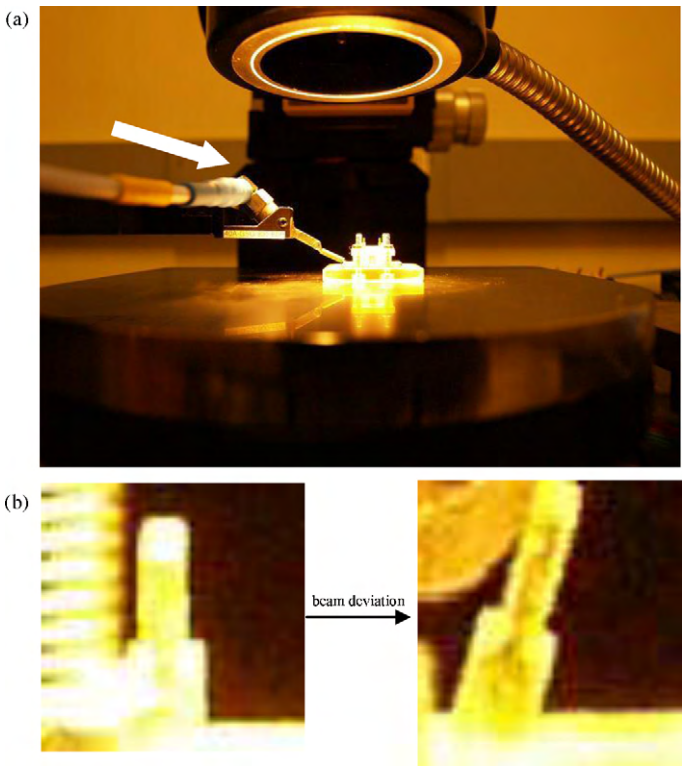

Fig. 5. Measurement setup for the beam deflection and resonance frequency: (a) measurement setup and (b) beam deflection.

$$S_{mechanical} \equiv \frac{\Delta\theta_{beam}}{\Delta v_{airflow}} \tag{7}$$

According to Eqs. (5)–(7), the sensitivity of the sensor is composed of two parts: RF sensitivity S_{RF}, which is determined by the cavity resonator design and mechanical sensitivity $S_{mechanical}$, which is determined by the mechanical properties of the elastic membrane and beam structures.

Firstly, a measurement of S_{RF} is performed by using an Agilent 8510C network analyzer. The S11 measurement shows a deep notch at the resonant frequency of the evanescent-mode cavity resonator, indicating a strong resonance. Fig. 5 shows the experimental setup. The beam is deflected by gently applying a horizontal force. Then, both the deflecting angle and the resonant frequency are recorded simultaneously. The dynamic range of the sensor is decided by the maximum deflection angle where the top membrane touches the capacitive post to have an electrical short. Fig. 6 shows the changes of simulated and measured resonant frequencies as a function of the beam deflection. The simulated curve is based on Eq. (6). The sensitivity varies with the deflection angle, and increases to an approximate maximum of 1.5 GHz/° when the deflection angle is close to the limit.

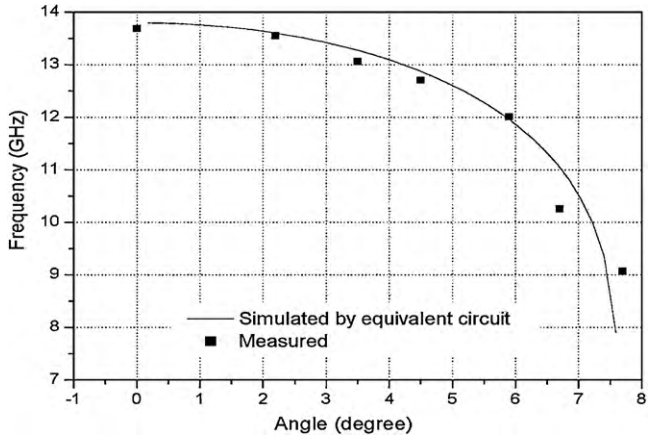

Fig. 6. RF measurement results of the airflow sensor: resonance frequency vs. beam angles.

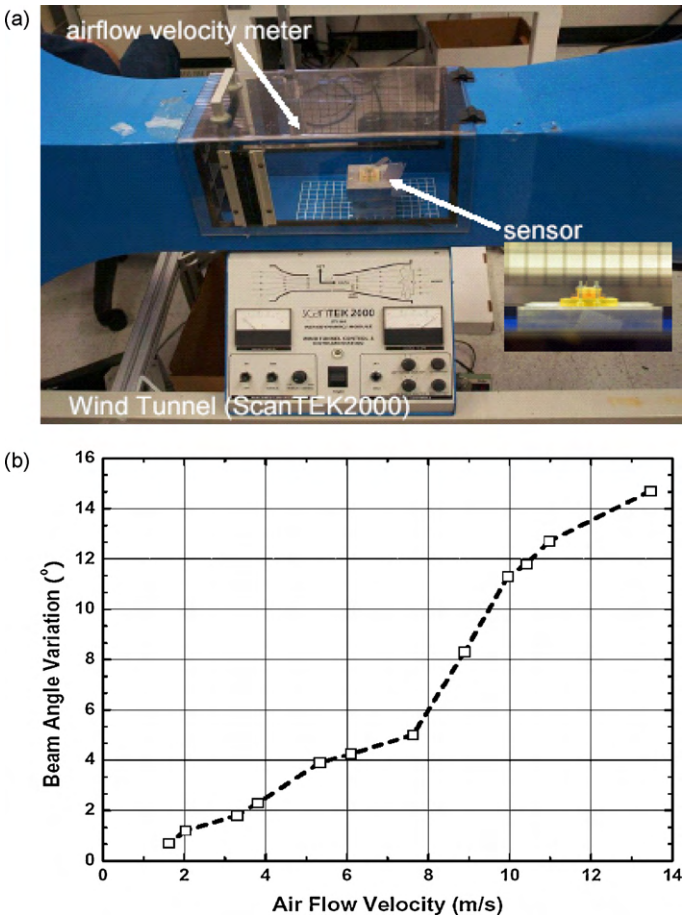

Fig. 7. Wind tunnel measurement setup and measured deflection angle vs. airflow velocity: (a) wind-tunnel measurement setup and (b) measurement data.

Knowledge of the velocity-deformation relations of the resonant cavity allows the transduction of flow velocities to resonant frequencies. The sensor is then put in a wind tunnel to characterize the airflow response. Fig. 7 shows the experimental setup of the wind tunnel (ScanTEK2000) and measurement results (Fig. 7(b)).

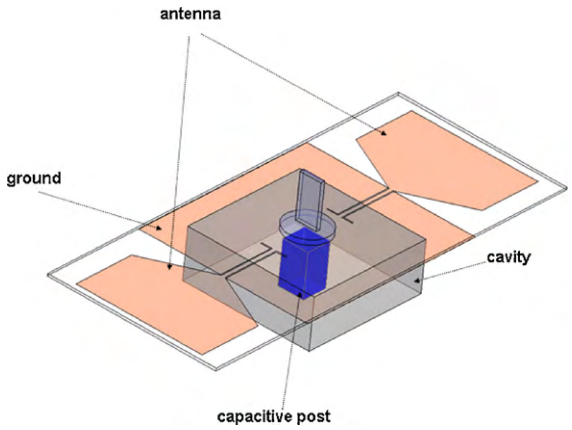

Fig. 8. Design schematic of a passive wireless displacement sensor.

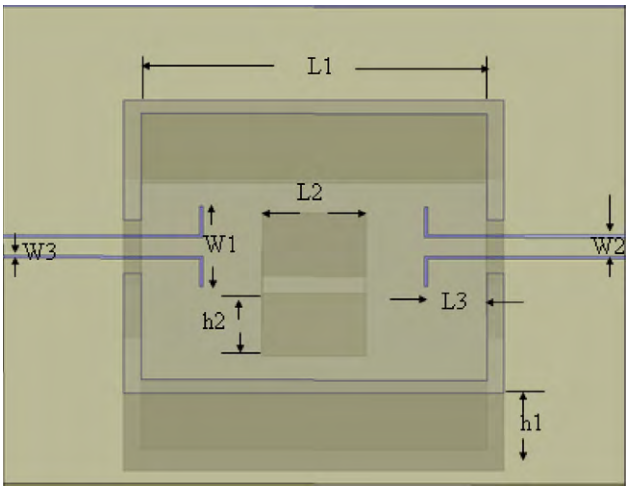

Fig. 9. Schematic design for the cavity resonator.

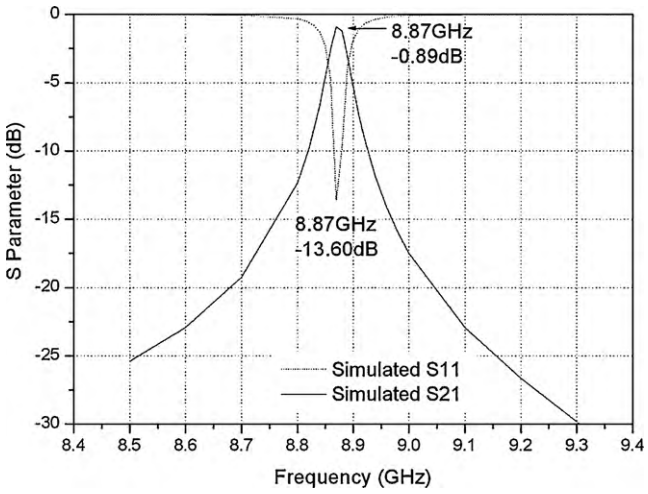

Fig. 10. Simulation results for the rectangular cavity resonator.

Table 2
Design parameters of cavity resonator for wireless interrogation.

$L1$ = 10.00 mm	$L2$ = 3.00 mm	$H1$ = 2.70 mm	$H2$ = 2.44 mm
$W1$ = 3.00 mm	$W2$ = 0.70 mm	$W3$ = 0.10 mm	$L3$ = 3.63 mm

When the airflow is applied to the sensor, the beam deflection angle is recorded. Meanwhile, the airflow velocity is measured using a reference flow velocity meter (FMA-605-I, OMEGA). The deflection angle has an approximately linear relation to the airflow velocity when the velocity is below 7.8 m/s. The nonlinear relation beyond 7.8 m/s is mostly due to the contact of the top membrane with the capacitive post inside the cavity. An approximate 1.4 (m/s)/° change of the beam angle can be observed in the linear region, *i.e.*, an equivalent sensitivity of larger than 0.37 GHz/(m/s) has been achieved for the airflow velocity sensing by the evanescent cavity resonator based sensor. The sensitivity or dynamic range can be easily adjusted by controlling membrane thickness or sensing beam dimension in order to meet requirements of specific applications.

4. Wireless interrogation design

To realize passive remote sensing, an antenna needs to be integrated with the cavity resonator. Connection of waveguide or cavity with antenna is usually achieved by hybrid integration using Sub-Miniature-version-A (SMA) connectors and cables, which is bulky in overall size. In this paper, the evanescent-mode cavity resonator is monolithically integrated with an external compact antenna for wireless interrogation. Fig. 8 shows a design schematic of a passive wireless sensor with the antenna for wireless sensing of normal directional displacement. A rectangular cavity resonator is connected with two sensor antennas via CPW transmission lines. Ultra-wide-bandwidth (UWB) monopole antenna is adopted as the sensor antenna for its compactness, wide bandwidth and omni-directional radiation pattern [20] and utilized to receive and transmit RF signals wirelessly.

Similar to the previous airflow sensor, the coupling from the CPW to cavity resonator can be enhanced by adjusting the CPW insertion length into the cavity. Fig. 9 shows the design of the cavity resonator with CPW transition. The design parameters are shown in Table 2.

Fig. 10 shows the HFSS full wave analysis results, indicating that the proposed CPW structure enables a low transition loss inside cavity less than 0.9 dB at resonance. The resonant frequency of the cavity resonator is designed at 8.87 GHz. The substrate in design is liquid crystal polymer (LCP) with $\varepsilon_r = 3.1$, and $\delta = 0.002$. A narrow bandwidth of 0.58% can be achieved for the cavity resonator. The UWB antenna is designed to have a wide 10 dB bandwidth from 5 to 20 GHz, enables a high dynamic range for the wireless detection.

The fabricated device is shown in Fig. 11. The evanescent-mode resonator is fabricated by molding epoxy resin and the sensor antenna is fabricated on LCP substrate by using photolithography.

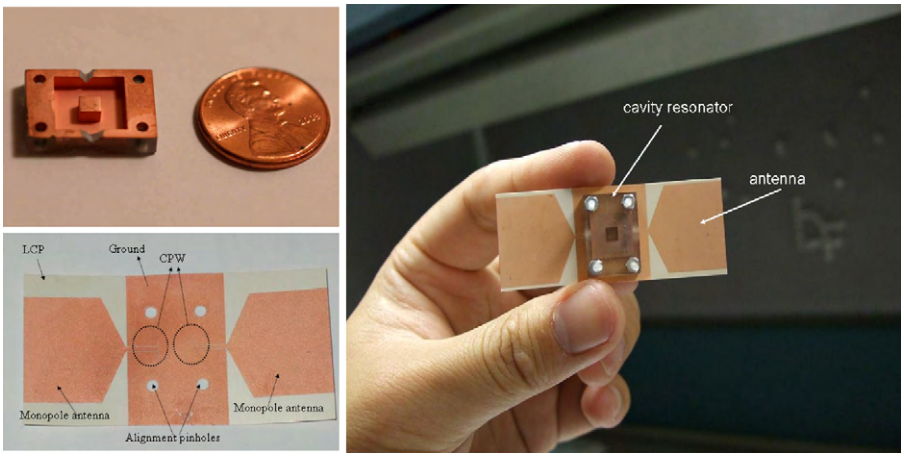

Fig. 11. Fabricated passive wireless displacement sensor.

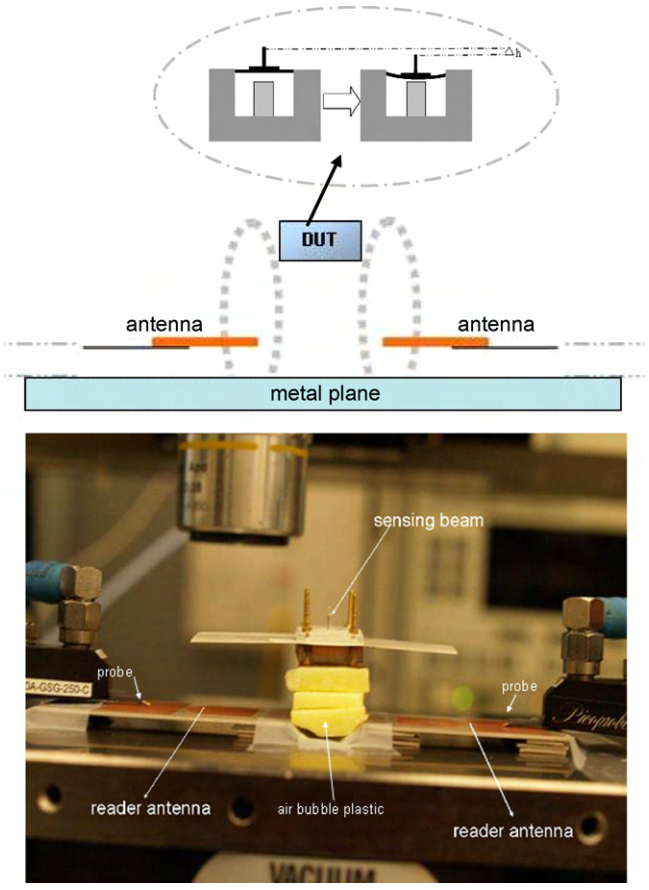

Fig. 12. Wireless interrogation measurement setup.

Both the resonator and sensor antenna are assembled using a fixture for ease of integration and testing.

Fig. 12 shows the wireless interrogation setup. Two external reader antennas are put head to head on the stage, while one works as a transmitting antenna and the other one works as a receiving antenna. Both reader antennas have estimated gain of 2 dBi at 8–10 GHz and have null radiation in horizontal direction to minimize the direct interference. The sensor is placed above the reader antennas by using a bubble plastic frame with dielectric constant close to air. The distance between the sensor and reader antennas is about 2 cm, well above near field distance at this frequency. Larger interrogation distance should be achieved if we use high gain reader antenna, such as a horn antenna. The sensor antenna reflects the interrogation signal to the receiving reader antenna in a similar way as RF backscattering. The resonance can be detected by measuring the S21 parameter from the two reader antennas. A vertical force is applied to the sensing beam to generate a displacement to change the sensor resonance frequency.

The S21 parameters are measured for the aforementioned wireless sensor setup, as shown in Fig. 13. The beam displacement is recorded and measured by a camera via microscope. When there is zero force on the beam, the measurement shows the resonance at about 8.85 GHz as predicted. However, the resonant frequency significantly changes when the beam is displaced. The measured curve of the resonant frequency versus the vertical displacement of the beam is shown in Fig. 14. The results indicate a sensitivity of 16.7 MHz/μm for the wireless displacement measurement. In the experiment, the interrogation distance is limited in near field due to the small power generated by the network analyzer. However, the interrogation distance can be further increased to far field with help of low noise amplifier (LNA) in the reader system.

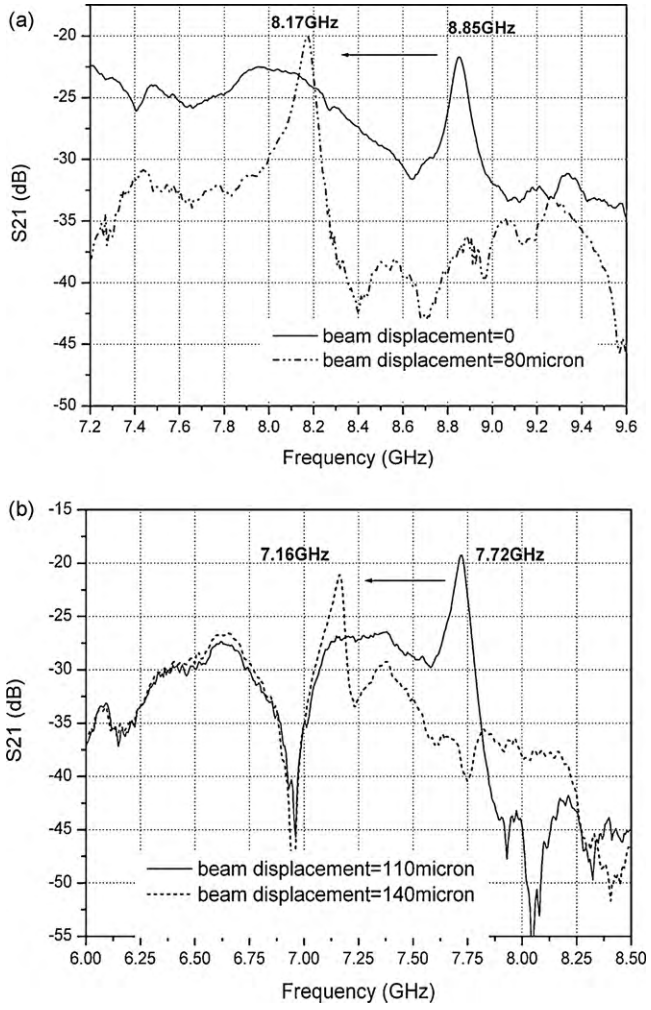

Fig. 13. Measured S21 by wireless interrogation for: (a) beam displacement = 0 and 80 μm and (b) beam displacement = 110 and 140 μm.

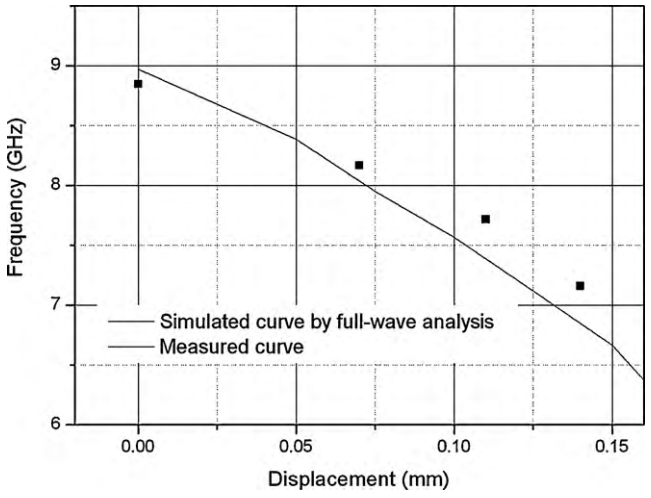

Fig. 14. Measured resonant frequency by wireless interrogation vs. beam displacement.

5. Conclusion

In this paper, a wireless passive sensing technique based on evanescent-mode cavity resonator has been successfully demonstrated for airflow and displacement measurements. By integrating

an UWB monopole antenna, the capability of passive wireless interrogation is also demonstrated. Micro-molding process has been exploited to fabricate the proposed sensor including the cavity resonator as well as the integrated CPW feeding structure. The proposed sensor technique is general enough to be implemented to more applications with low power sensor network. The simple resonator structure can also fabricated by metal or ceramics, enabling the applications for high temperature or other harsh working environments.

References

[1] M.G. Allen, Micromachined endovascularly-implantable wireless aneurysm pressure sensor: from concept to clinic, Proc. Transducers (2005) 275–278.
[2] A.D. DeHennis, K.D. Wise, A fully integrated multisite pressure sensor for wireless arterial flow characterization, J. Microelectromech. Syst. 15 (3) (2006) 678–685.
[3] M.R. Shah, R.P. Phillips, R.A. Normann, A study of printed spiral coils for neuroprosthetic transcranial telemetry applications, IEEE Trans. Biomed. Eng. 45 (7) (1998) 867–876.
[4] T. Ohki, J. Yadav, N. Gargiulo, H. Kurvers, S. Rhee, F.J. Veith, D. Stern, Preliminary results of an implantable wireless aneurysm pressure sensor in a canine model: Will surveillance CT scan following EVAR become obsolete? J. Endovasc. Ther. 10 (2003) 1–32.
[5] M.A. Fonseca, J.M. English, M. von Arx, M.G. Allen, Wireless micromachined ceramic pressure sensor for high temperature applications, IEEE J. Microelectromech. Syst. 11 (4) (2002) 337–343.
[6] L. Reindl, G. Scholl, T. Ostertag, C.C.W. Ruppel, W.-E. Bulst, F. Seifert, SAW devices as wireless passive sensors, in: Proceedings of the IEEE Ultrasonics Symposium, 1996, pp. 363–367.
[7] T. Sachs, R. GroBmann, J. Michel, E. Schrtlfer, Remote sensing using quartz sensors, Proc. SPIE 2718 (1996) 47–58.
[8] J. Chuang, D.J. Thomson, G.E. Bridges, Embeddable wireless strain sensor based on resonant RF cavities, Rev. Sci. Instrum. 76 (2005) 094703.
[9] G.F. Craven, C.K. Mok, The design of evanescent mode waveguide bandpass filters for a prescribed insertion loss characteristic, IEEE Trans. Microwave Theory Tech. 19 (3) (1971) 295–308.
[10] C.K. Mok, Design of evanescent mode waveguide diplexers, IEEE Trans. Microwave Theory Tech. 21 (1) (1973) 43–48.
[11] R.V. Snyder, new application of evanescent mode waveguide to filter design, IEEE Trans. Microwave Theory Tech. 25 (12) (1977) 1013–1021.
[12] X. Gong, A. Margomenos, B. Liu, S. Hajela, L.P.B. Katehi, W.J. Chappell, Precision fabrication techniques and analysis on high-Q evanescent-mode resonators and filters of different geometries, IEEE Trans. Microwave Theory Tech. 52 (11) (2004) 2557–2566.
[13] H. Joshi, H.H. Sigmarsson, D. Peroulis, W.J. Chappell, Highly loaded evanescent cavities for widely tunable high-Q filters, in: IEEE/MTT-S International, 2007, pp. 2133–2136.
[14] A. Mahmood, H.H. Sigmarsson, H. Joshi, W.J. Chappell, D. Peroulis, An evanescent-mode cavity resonator based thermal sensor, in: Proceedings of the IEEE Sensors, 2007, pp. 950–953.
[15] B. Pan, Y. Li, M.M. Tentzeris, J. Papapolymerou, A high-Q millimeter-wave air-lifted cavity resonator on lossy substrates, IEEE Microwave Wireless Comp. Lett. 17 (8) (2007) 571–573.
[16] Y. Li, B. Pan, M.M. Tentzeris, J. Papapolymerou, A fully micromachined W-band coplanar waveguide to rectangular waveguide transition, in: Proceedings of the IEEE-IMS Symposium, 2007, pp. 1031–1034.
[17] Y. Zhao, Y.-K. Yoon, M.G. Allen, Metal-transfer-micromolded RF components for system-on-package (SOP), in: Proceedings of the Electronic Components and Technology Conference, 2007, pp. 1877–1883.
[18] Y. Zhao, Y.-K. Yoon, X. Wu, M.G. Allen, Metal-transfer-micromolding of air-lifted RF components, Proc. Transducers (2007) 659–663.
[19] Y. Zhao, S.-H. Kim, Y. Li, B. Pan, X. Wu, M. Tentzeris, J. Papapolymerou, M.G. Allen, A micromachined airflow sensor based on RF evanescent-mode cavity resonator, in: IEEE-IMS Symposium, 2008, pp. 1199–1203.
[20] M. Yanagi, S. Kurashima, T. Arita, T. Kobayashi, Planar UWB Monopole Antenna Formed on a Printed Circuit Board, Fujitsu Component Limited, http://www.fcai.fujitsu.com/pdf/uwb_monopole_ antenna.pdf.